ISSN 1674-1056
http://cpb.iphy.ac.cn
http://iopscience.iop.org/cpb
中国物理 B
Chinese Physics
中国物理
Chinese Physics B

Influence of moderate-to-strong anisotropic non-Kolmogorov turbulence on intensity fluctuations of a Gaussian-Schell model beam in marine atmosphere

Mingjian Cheng(程明建), Lixin Guo(郭立新), Jiangting Li(李江挺)
Citation: Chin. Phys. B . 2018, 27(5): 054203. **doi:** 10.1088/1674-1056/27/5/054203

Journal homepage: http://cpb.iphy.ac.cn; http://iopscience.iop.org/cpb

What follows is a list of articles you may be interested in

A new method of calculating the orbital angular momentum spectra of Laguerre-Gaussian beams in channels with atmospheric turbulence

Xiao-zhou Cui(崔小舟), Xiao-li Yin(尹霄丽), Huan Chang(常欢), Zhi-chao Zhang(张志超), Yong-jun Wang(王拥军), Guo-hua Wu(吴国华)
Chin. Phys. B . 2017, 26(11): 114207. **doi:** 10.1088/1674-1056/26/11/114207

Propagation factor of electromagnetic concentric rings Schell-model beams in non-Kolmogorov turbulence

Zhen-Zhen Song(宋真真), Zheng-Jun Liu(刘正君), Ke-Ya Zhou(周可雅), Qiong-Ge Sun(孙琼阁), Shu-Tian Liu(刘树田)
Chin. Phys. B . 2017, 26(2): 024201. **doi:** 10.1088/1674-1056/26/2/024201

Optimizing calculation of phase screen distribution with minimum condition along an inhomogeneous turbulent path

Wen-Yi Shao(邵文毅), Hao Xian(鲜浩)
Chin. Phys. B . 2016, 25(11): 114212. **doi:** 10.1088/1674-1056/25/11/114212

Turbulence mitigation scheme based on multiple-user detection in an orbital-angular-momentum multiplexed system

Li Zou(邹丽), Le Wang(王乐), Sheng-Mei Zhao(赵生妹), Han-Wu Chen(陈汉武)
Chin. Phys. B . 2016, 25(11): 114215. **doi:** 10.1088/1674-1056/25/11/114215

Scintillation of partially coherent Gaussian-Schell model beam propagation in slant atmospheric turbulence considering inner- and outer-scale effects

Li Ya-Qing, Wu Zhen-Sen, Zhang Yuan-Yuan, Wang Ming-Jun
Chin. Phys. B . 2014, 23(7): 074202. **doi:** 10.1088/1674-1056/23/7/074202

Influence of moderate-to-strong anisotropic non-Kolmogorov turbulence on intensity fluctuations of a Gaussian–Schell model beam in marine atmosphere*

Mingjian Cheng(程明建)[1,2], Lixin Guo(郭立新)[1,†], and Jiangting Li(李江挺)[1]

[1] School of Physics and Optoelectronic Engineering, Xidian University, Xi'an 710071, China
[2] State Key Laboratory of Pulsed Power Laser Technology, Hefei 230037, China

(Received 9 October 2017; revised manuscript received 8 January 2018; published online 26 April 2018)

The scintillation index (SI) of a Gaussian–Schell model (GSM) beam in a moderate-to-strong anisotropic non-Kolmogorov turbulent atmosphere is developed based on the extended Rytov theory. The on-axis SI in a marine atmosphere is higher than that in a terrestrial atmosphere, but the off-axis SI exhibits the opposite trend. The on-axis SI first increases and then begins to decrease and saturate as the turbulence strength increases. Turbulence inner and outer scales have different effects on the on-axis SI in different turbulent fluctuation regions. The anisotropy characteristic of atmospheric turbulence leads to the decline in the on-axis SI, and the rise in the off-axis SI. The on-axis SI can be lowered by increasing the anisotropy of turbulence, wavelength, and source partial coherence before entering the saturation attenuation region. The developed model may be useful for evaluating ship-to-ship/shore free-space optical communication system performance.

Keywords: atmospheric turbulence, Gaussian–Schell model beam, scintillation, atmospheric propagation

PACS: 42.25.Dd, 42.25.Kb, 42.68.Bz, 92.60.hk **DOI:** 10.1088/1674-1056/27/5/054203

1. Introduction

Research on the propagation behavior of laser beams through atmospheric turbulence is of significant importance in various applications, including free-space optical (FSO) communications, imaging systems, and remote sensing.[1] Atmospheric turbulence produces several negative effects that can severely degrade these systems' performance, of which the most noticeable is the intensity fluctuation, known as scintillation.[2] To mitigate these turbulence effects, considerable effort has been put into partially coherent beams.[3,4] Both theory and experiment show that partially coherent beams have a significant advantage over fully coherent ones in mitigating turbulence-induced scintillation.[5,6] The Gaussian–Schell model (GSM) beam is an important member of the partially coherent beams, whose amplitude distribution and spatial coherence function are both Gaussian shapes. It can be easily generated by passing through the phase diffusers at the laser transmitter. Over the past decades, the irradiance scintillation index (SI) for Gaussian beams under weak and moderate-to-strong turbulence regimes has been developed,[7–12] and employed to examine the performance of FSO communication systems based on GSM beams.[13–15] However, these studies mainly focused on the isotropic Kolmogorov or non-Kolmogorov terrestrial atmospheric turbulence.

With increasing activities and communication needs in the marine environment, it is essential to understand the turbulent effects in the marine atmosphere. The SI of a laser beam in a marine atmosphere is relatively less explored compared to that in a terrestrial atmosphere. In the marine atmosphere, large bodies of water act differently from soils,[16] which makes the marine atmospheric turbulence behave differently from the terrestrial atmospheric turbulence. The statistical models derived for terrestrial atmospheric turbulence cannot be applied directly to marine atmospheric turbulence. A new power spectrum of marine atmospheric turbulence was proposed and used to develop the SI models for plane waves, spherical waves, and higher-order laser beams in a weak Kolmogorov turbulent marine atmosphere.[17–19] The non-Kolmogorov marine atmospheric turbulence spectrum has been adopted to analyze the SI of a Gaussian beam in a weak marine atmospheric turbulence.[20] Due to the sea surface friction on the air motion, optical turbulence in a marine atmosphere can be anisotropic. The polarization, beam wander, and spreading of Gaussian–Schell model beams propagating in an anisotropic non-Kolmogorov turbulent marine atmosphere were investigated.[21,22] In 2016, Cui developed the SI of Gaussian beams through weak anisotropic non-Kolmogorov turbulence.[23] To the best of our knowledge, the SI of partially coherent GSM beams in moderate-to-strong anisotropic non-Kolmogorov marine atmospheric turbulence has never been examined.

*Project supported by the Open Research Fund of State Key Laboratory of Pulsed Power Laser Technology (Grant No. SKL2016KF05), the Key Industrial Innovation Chain Project in Industrial Domain, China (Grant No. 2017ZDCXL-GY-06-02), the Huawei Innovation Research Program, China (Grant No. HO2017050001AG), and the Foundation for Innovative Research Groups of the National Natural Science Foundation of China (Grant No. 61621005).

†Corresponding author. E-mail: lxguo@xidian.edu.cn

© 2018 Chinese Physical Society and IOP Publishing Ltd

In this paper, the on-axis and off-axis SIs of a GSM beam through a moderate-to-strong anisotropic non-Kolmogorov marine atmosphere are developed by adopting the extended Rytov theory. The influences of the anisotropy coefficient, power-spectrum index, turbulence inner-, outer-scales, turbulence structure parameter, off-axis distance, propagation distance, spatial correlation length, wavelength, and beam width on the SIs of GSM beams are discussed in detail.

2. Theory

Based on the extended Rytov theory, the effective anisotropic non-Kolmogorov modified atmospheric spectrum model can be expressed as[11]

$$\Phi_{n,\mathrm{M}}(\kappa,\alpha)=\Phi_n(\kappa,\alpha)\left[G_x(\kappa,\alpha)+G_y(\kappa,\alpha)\right],\ \ 3<\alpha<4, \tag{1}$$

where $\Phi_n(\kappa,\alpha)$ represents the anisotropic non-Kolmogorov spectrum over the inertial sub-range[24]

$$\Phi_n(\kappa,\alpha)=A(\alpha)\mu^{2-\alpha}\tilde{C}_n^2\kappa^{-\alpha},\quad \kappa=\sqrt{\kappa_x^2+\kappa_y^2+\kappa_z^2}, \tag{2}$$

where $\tilde{C}_n^2$ is the generalized refractive-index structure parameter with units $\mathrm{m}^{3-\alpha}$, μ denotes the anisotropy coefficient, α is the power-spectrum index, $A(\alpha)$ is a constant that maintains consistency between the refractive-index structure function and its power spectrum that has the form $A(\alpha)=\Gamma(\alpha-1)\sin[(\alpha-3)\pi/2]/(4\pi^2)$ with symbol $\Gamma(\cdot)$ being the Gamma function.[25] When $\alpha=11/3$ and $\mu=1$, equation (2) reduces to the standard Kolmogorov spectrum model.

The high-pass filter function of small-scale $G_y(\kappa,\alpha)$ and low-pass filter function of large-scale $G_x(\kappa,\alpha)$ can be written as

$$G_y(\kappa,\alpha)=\exp\left(\Lambda\kappa^2\xi^2/k\right)\kappa^{\alpha}/\left(\kappa_\mu^2+\kappa_y^2\right)^{\alpha/2},\ \ \kappa_y\gg 1, \tag{3}$$

$$G_x(\kappa,\alpha)=\left[1-\exp\left(-\frac{\kappa_\mu^2}{\kappa_0^2}\right)\right]\exp\left(-\frac{\kappa_\mu^2}{\kappa_l^2}-\frac{\kappa_\mu^2}{\kappa_x^2}\right)\times\left[1+a_1\left(\frac{\kappa_\mu}{\kappa_l}\right)+a_2\left(\frac{\kappa_\mu}{\kappa_l}\right)^{3-\alpha/2}\right], \tag{4}$$

where $\kappa_\mu=\sqrt{\kappa_z^2+\mu^2\kappa_{xy}^2}$. In the marine atmosphere, $a_1=-0.061$, $a_2=2.836$, and in terrestrial atmosphere, $a_1=1.802$, $a_2=-0.254$. Specifically, the parameter κ_x is a large-scale (or refractive) cutoff spatial frequency for the large-scale turbulent cells, and κ_y is a small-scale (or diffractive) cutoff spatial frequency for the small-scale turbulent cells. $\kappa_l=c_0/l_0$, $\kappa_0=8\pi/L_0$, l_0, and L_0 are turbulence inner-scale and outer-scale; parameter c_0 has the form of[20]

$$c_0=\left\{\pi A(\alpha)\left[\Gamma\left(\frac{3}{2}-\frac{\alpha}{2}\right)\frac{3-\alpha}{3}+a_1\Gamma\left(2-\frac{\alpha}{2}\right)\frac{4-\alpha}{3}+a_2\Gamma\left(3-\frac{3\alpha}{4}\right)\frac{4-\alpha}{2}\right]\right\}^{1/\alpha-5}. \tag{5}$$

The total SI of a GSM beam propagation in the turbulent atmosphere is composed of radial (off-axis) and longitudinal (on-axis) components[2]

$$\delta_{\mathrm{I}}^2(r,L)=\delta_{\mathrm{I,l}}^2(L)+\delta_{\mathrm{I,r}}^2(r,L), \tag{6}$$

where

$$\delta_{\mathrm{I,l}}^2(L)=16\pi^2k^2L\int_0^1\int_0^\infty\kappa\Phi_{n,\mathrm{M}}(\kappa,\alpha)\exp\left(-\Lambda_{\mathrm{e}}L\kappa^2\xi^2/k\right)\times\sin^2\left[L\kappa^2\xi\left(1-\bar{\Theta}_{\mathrm{e}}\xi\right)/(2k)\right]\mathrm{d}\kappa\mathrm{d}\xi, \tag{7}$$

$$\delta_{\mathrm{I,r}}^2(r,L)=8\pi^2k^2L\int_0^1\int_0^\infty\kappa\Phi_{n,\mathrm{M}}(\kappa,\alpha)\exp\left(-\Lambda_{\mathrm{e}}L\kappa^2\xi^2/k\right)\times\left[I_0\left(2\Lambda_{\mathrm{e}}r\kappa\xi\right)-1\right]\mathrm{d}\kappa\mathrm{d}\xi, \tag{8}$$

where $k=2\pi/\lambda$ is the wavenumber with λ being wavelength, $I_0(x)$ is a modified Bessel function of the first kind; L is the propagation distance, ξ is the normalized path coordinate and related to z by $\xi=z/L$; r is the off-axis parameter; the complementary parameter $\bar{\Theta}_{\mathrm{e}}=1-\Theta_{\mathrm{e}}$s, Θ_{e} and Λ_{e}, are effective output beam parameters of GSM beams, that are related to the input beam parameters Θ_0 and Λ_0 of Gaussian beams[2]

$$\Theta_{\mathrm{e}}=\Theta_0/\left(\Theta_0^2+\Lambda_0^2\zeta_{\mathrm{s}}\right),\quad \Lambda_{\mathrm{e}}=\Lambda_0\zeta_{\mathrm{s}}/\left(\Theta_0^2+\Lambda_0^2\right), \tag{9}$$

where Θ_0 and Λ_0 are defined by $\Theta_0=1-L/F$ and $\Lambda_0=2L/\left(kw_0^2\right)$, respectively. Here, F and w_0 denote the phase front radius of curvature and beam radius at the input plane, respectively. $\zeta_{\mathrm{s}}=1+4q_{\mathrm{c}}/\Lambda_0=1+w_0^2/l_{\mathrm{s}}^2$ is the source coherence parameter of the GSM beam (if $\zeta_{\mathrm{s}}=1$, the beam is fully coherent, if $\zeta_{\mathrm{s}}>1$, the beam is partially coherent), and l_{s} is the partial coherence length, which describes the partial coherence properties of the source.

The on-axis SI of GSM beam propagation in moderate-to-strong anisotropic non-Kolmogorov turbulence takes the following form:

$$\delta_{\mathrm{I,l}}^2(L)=\exp\left(\delta_{\ln x,l}^2+\delta_{\ln y,l}^2\right)-1, \tag{10}$$

where $\delta_{\ln x,l}^2$ and $\delta_{\ln y,l}^2$ are large-scale and small-scale log-irradiance on-axis SIs of GSM beams, respectively, and given by

$$\delta_{\ln x,l}^2=16\pi^2k^2L\int_0^1\int_0^\infty\kappa\Phi_n(\kappa,\alpha)G_x(\kappa)\exp\left(-\frac{\Lambda_{\mathrm{e}}L\kappa^2\xi^2}{k}\right)\times\sin^2\left[\frac{L\kappa^2\xi\left(1-\bar{\Theta}_{\mathrm{e}}\xi\right)}{2k}\right]\mathrm{d}\kappa\mathrm{d}\xi, \tag{11}$$

$$\delta_{\ln y,l}^2=16\pi^2k^2L\int_0^1\int_0^\infty\kappa\Phi_n(\kappa,\alpha)G_y(\kappa)\exp\left(-\frac{\Lambda_{\mathrm{e}}L\kappa^2\xi^2}{k}\right)\times\sin^2\left[\frac{L\kappa^2\xi\left(1-\bar{\Theta}_{\mathrm{e}}\xi\right)}{2k}\right]\mathrm{d}\kappa\mathrm{d}\xi. \tag{12}$$

For large-scale log-irradiance on-axis SI, we use the geometrical optics approximation of $\sin x\approx x$, equation (11) can be expressed as the difference, viz.,

$$\delta_{\ln x,l}^2=\delta_{\ln x,l}^2(l_0)-\delta_{\ln x,l}^2(L_0), \tag{13}$$

where

$$\begin{aligned}\delta^2_{\ln x,l}(l_0) &= 2\pi^2 A(\alpha)\left[1.23R(\alpha)\right]^{-1}\delta_{\rm R}^2\mu^{2-\alpha}\\ &\times\int_0^1\int_0^\infty\left[1+a_1\left(\eta\eta_l^{-1}\right)^{1/2}+a_2\left(\eta\eta_l^{-1}\right)^{3/2-\alpha/4}\right]\\ &\times\xi^2\left(1-\bar{\Theta}_{\rm e}\xi\right)^2\eta^{2-\alpha/2}\\ &\times\exp\left[-\left(\Lambda_{\rm e}\xi^2+\eta_x^{-1}+\eta_l^{-1}\right)\eta\right]{\rm d}\eta{\rm d}\xi,\end{aligned}\tag{14}$$

$$\begin{aligned}\delta^2_{\ln x,l}(L_0) &= 2\pi^2 A(\alpha)\left[1.23R(\alpha)\right]^{-1}\delta_{\rm R}^2\mu^{2-\alpha}\\ &\times\int_0^1\int_0^\infty\left[1+a_1\left(\eta\eta_l^{-1}\right)^{1/2}+a_2\left(\eta\eta_l^{-1}\right)^{3/2-\alpha/4}\right]\\ &\times\xi^2\left(1-\bar{\Theta}_{\rm e}\xi\right)^2\eta^{2-\alpha/2}\\ &\times\exp\left[-\left(\Lambda_{\rm e}\xi^2+\eta_x^{-1}+\eta_l^{-1}+\eta_0^{-1}\right)\eta\right]{\rm d}\eta{\rm d}\xi,\end{aligned}\tag{15}$$

where

$$\delta_{\rm R}^2 = R(\alpha)\times\delta_{\rm Rytov}^2 = \frac{-6.5\pi^2 A(\alpha)}{\alpha}\Gamma\left(1-\frac{\alpha}{2}\right)\sin\left(\alpha\frac{\pi}{4}\right)\times 1.23\tilde{C}_n^2 k^{3-\frac{\alpha}{2}}L^{\frac{\alpha}{2}}$$

is the SI of a plane wave in weak non-Kolmogorov turbulence, $\eta = L\kappa^2/k$, $\eta_l = L\kappa_l^2/\left(k\mu^2\right)$, $\eta_x = L\kappa_x^2/\left(k\mu^2\right)$, $\eta_0 = L\kappa_0^2/\left(k\mu^2\right)$.

Based on the integrals,[26]

$$\int_0^\infty {\rm e}^{-s\eta}\eta^{x-1}{\rm d}\eta = \Gamma(x)/s^x,\tag{16}$$

and

$${}_2{\rm F}_1(a,b;c;z) = \frac{\Gamma(c)}{\Gamma(b)\Gamma(c-b)}\int_0^1 t^{b-1}(1-t)^{c-b-1}\times(1-zt)^{-a}{\rm d}t,\quad c>b>0,\tag{17}$$

equation (14) becomes

$$\begin{aligned}\delta^2_{\ln x,l}(l_0) &= \frac{2\pi^2A(\alpha)}{1.23R(\alpha)}\delta_{\rm R}^2\mu^{2-\alpha}\hat{\eta}_x^{3-\alpha/2}\left\{\Gamma\left(3-\frac{\alpha}{2}\right)\left[\frac{1}{3}{}_2{\rm F}_1\left(3-\frac{\alpha}{2},\frac{3}{2};\frac{5}{2};-\Lambda_{\rm e}\hat{\eta}_x\right)-\frac{\bar{\Theta}_{\rm e}}{2}{}_2{\rm F}_1\left(3-\frac{\alpha}{2},2;3;-\Lambda_{\rm e}\hat{\eta}_x\right)\right.\right.\\ &+\left.\frac{\bar{\Theta}_{\rm e}^2}{5}{}_2{\rm F}_1\left(3-\frac{\alpha}{2},\frac{5}{2};\frac{7}{2};-\Lambda_{\rm e}\hat{\eta}_x\right)\right]+a_1\Gamma\left(\frac{7}{2}-\frac{\alpha}{2}\right)\left(\frac{\hat{\eta}_x}{\eta_l}\right)^{1/2}\left[\frac{1}{3}{}_2{\rm F}_1\left(\frac{7}{2}-\frac{\alpha}{2},\frac{3}{2};\frac{5}{2};-\Lambda_{\rm e}\hat{\eta}_x\right)\right.\\ &-\frac{\bar{\Theta}_{\rm e}}{2}{}_2{\rm F}_1\left(\frac{7}{2}-\frac{\alpha}{2},2;3;-\Lambda_{\rm e}\hat{\eta}_x\right)+\left.\frac{\bar{\Theta}_{\rm e}^2}{5}{}_2{\rm F}_1\left(\frac{7}{2}-\frac{\alpha}{2},\frac{5}{2};\frac{7}{2};-\Lambda_{\rm e}\hat{\eta}_x\right)\right]+a_2\Gamma\left(\frac{9}{2}-\frac{3\alpha}{4}\right)\left(\frac{\hat{\eta}_x}{\eta_l}\right)^{3/2-\alpha/4}\\ &\times\left.\left[\frac{1}{3}{}_2{\rm F}_1\left(\frac{9}{2}-\frac{3\alpha}{4},\frac{3}{2};\frac{5}{2};-\Lambda_{\rm e}\hat{\eta}_x\right)-\frac{\bar{\Theta}_{\rm e}}{2}{}_2{\rm F}_1\left(\frac{9}{2}-\frac{3\alpha}{4},2;3;-\Lambda_{\rm e}\hat{\eta}_x\right)+\frac{\bar{\Theta}_{\rm e}^2}{5}{}_2{\rm F}_1\left(\frac{9}{2}-\frac{3\alpha}{4},\frac{5}{2};\frac{7}{2};-\Lambda_{\rm e}\hat{\eta}_x\right)\right]\right\}.\end{aligned}\tag{18}$$

Analogously, equation (15) can be expressed as

$$\begin{aligned}\delta^2_{\ln x,l}(L_0) &= \frac{2\pi^2A(\alpha)}{1.23R(\alpha)}\delta_{\rm R}^2\mu^{2-\alpha}\hat{\eta}_{x0}^{3-\alpha/2}\left\{\Gamma\left(3-\frac{\alpha}{2}\right)\left[\frac{1}{3}{}_2{\rm F}_1\left(3-\frac{\alpha}{2},\frac{3}{2};\frac{5}{2};-\Lambda_{\rm e}\hat{\eta}_{x0}\right)-\frac{\bar{\Theta}_{\rm e}}{2}{}_2{\rm F}_1\left(3-\frac{\alpha}{2},2;3;-\Lambda_{\rm e}\hat{\eta}_{x0}\right)\right.\right.\\ &+\left.\frac{\bar{\Theta}_{\rm e}^2}{5}{}_2{\rm F}_1\left(3-\frac{\alpha}{2},\frac{5}{2};\frac{7}{2};-\Lambda_{\rm e}\hat{\eta}_{x0}\right)\right]+a_1\Gamma\left(\frac{7}{2}-\frac{\alpha}{2}\right)\left(\frac{\hat{\eta}_{x0}}{\eta_l}\right)^{1/2}\left[\frac{1}{3}{}_2{\rm F}_1\left(\frac{7}{2}-\frac{\alpha}{2},\frac{3}{2};\frac{5}{2};-\Lambda_{\rm e}\hat{\eta}_{x0}\right)\right.\\ &-\left.\frac{\bar{\Theta}_{\rm e}}{2}{}_2{\rm F}_1\left(\frac{7}{2}-\frac{\alpha}{2},2;3;-\Lambda_{\rm e}\hat{\eta}_{x0}\right)+\frac{\bar{\Theta}_{\rm e}^2}{5}{}_2{\rm F}_1\left(\frac{7}{2}-\frac{\alpha}{2},\frac{5}{2};\frac{7}{2};-\Lambda_{\rm e}\hat{\eta}_{x0}\right)\right]\\ &+a_2\Gamma\left(\frac{9}{2}-\frac{3\alpha}{4}\right)\left(\frac{\hat{\eta}_{x0}}{\eta_l}\right)^{3/2-\alpha/4}\left[\frac{1}{3}{}_2{\rm F}_1\left(\frac{9}{2}-\frac{3\alpha}{4},\frac{3}{2};\frac{5}{2};-\Lambda_{\rm e}\hat{\eta}_{x0}\right)\right.\\ &-\left.\left.\frac{\bar{\Theta}_{\rm e}}{2}{}_2{\rm F}_1\left(\frac{9}{2}-\frac{3\alpha}{4},2;3;-\Lambda_{\rm e}\hat{\eta}_{x0}\right)+\frac{\bar{\Theta}_{\rm e}^2}{5}{}_2{\rm F}_1\left(\frac{9}{2}-\frac{3\alpha}{4},\frac{5}{2};\frac{7}{2};-\Lambda_{\rm e}\hat{\eta}_{x0}\right)\right]\right\},\end{aligned}\tag{19}$$

where ${}_2{\rm F}_1(a,\ b;\ c;\ x)$ is a hypergeometric function, $\hat{\eta}_x = \eta_l\eta_x/\left(\eta_x+\eta_l\right)$ and $\hat{\eta}_{x0} = \eta_x\eta_0\eta_l/\left(\eta_x\eta_0+\eta_x\eta_l+\eta_0\eta_l\right)$. When $\Lambda_{\rm e}\hat{\eta}_x \ll 1$, all the above hypergeometric functions are approximately equal to one, thus equations (18) and (19) reduce to

$$\begin{aligned}\delta^2_{\ln x,l}(l_0) &\approx \frac{2\pi^2A(\alpha)}{1.23R(\alpha)}\delta_{\rm R}^2\mu^{2-\alpha}\hat{\eta}_x^{3-\alpha/2}\left(\frac{1}{3}-\frac{\bar{\Theta}_{\rm e}}{2}+\frac{\bar{\Theta}_{\rm e}^2}{5}\right)\\ &\times\left[\Gamma\left(3-\frac{\alpha}{2}\right)+a_1\Gamma\left(\frac{7}{2}-\frac{\alpha}{2}\right)\left(\frac{\hat{\eta}_x}{\eta_l}\right)^{1/2}\right.\\ &+\left.a_2\Gamma\left(\frac{9}{2}-\frac{3\alpha}{4}\right)\left(\frac{\hat{\eta}_x}{\eta_l}\right)^{3/2-\alpha/4}\right],\end{aligned}\tag{20}$$

$$\begin{aligned}\delta^2_{\ln x,l}(L_0) &\approx \frac{2\pi^2A(\alpha)}{1.23R(\alpha)}\delta_{\rm R}^2\mu^{2-\alpha}\hat{\eta}_{x0}^{3-\alpha/2}\left(\frac{1}{3}-\frac{\bar{\Theta}_{\rm e}}{2}+\frac{\bar{\Theta}_{\rm e}^2}{5}\right)\\ &\times\left[\Gamma\left(3-\frac{\alpha}{2}\right)+a_1\Gamma\left(\frac{7}{2}-\frac{\alpha}{2}\right)\left(\frac{\hat{\eta}_{x0}}{\eta_l}\right)^{1/2}\right.\\ &+\left.a_2\Gamma\left(\frac{9}{2}-\frac{3\alpha}{4}\right)\left(\frac{\hat{\eta}_{x0}}{\eta_l}\right)^{3/2-\alpha/4}\right].\end{aligned}\tag{21}$$

Note that when $\mu = 1$, $l_0 \to 0$, $L_0 \to \infty$, equation (13)

reduces to

$$\delta^2_{\ln x,l} \approx \frac{2\pi^2 A(\alpha)}{1.23R(\alpha)}\delta^2_{\rm R}\eta_x^{3-\alpha/2}\left(\frac{1}{3}-\frac{\bar{\Theta}_{\rm e}}{2}+\frac{\bar{\Theta}_{\rm e}^2}{5}\right)\Gamma\left(3-\frac{\alpha}{2}\right), \quad (22)$$

which is the large-scale log-irradiance on-axis SI for the zero-scale case in the isotropic turbulent atmosphere.[11]

Along the same lines, we adopt the approximation of $1-\cos x \approx 1$ for the small-scale log-irradiance on-axis SI $\delta^2_{\ln y,l}$, and equation (12) can be written as

$$\begin{aligned}\delta^2_{\ln y,l} &= \frac{4\pi^2}{1.23}\frac{A(\alpha)}{R(\alpha)}\delta^2_{\rm R}\mu^{2-\alpha}\int_0^1\int_0^\infty\left(\frac{\eta_y}{\mu^2}+\eta\right)^{-\alpha/2}{\rm d}\eta{\rm d}\xi \\ &\approx \frac{8\pi^2}{1.23}\frac{A(\alpha)}{R(\alpha)}\frac{\delta^2_{\rm R}}{\alpha-2}\eta_y^{1-\alpha/2}, \end{aligned} \quad (23)$$

where $\eta_y = L\kappa_y^2/k$.

Similar to Ref. [11], the large-scale and small-scale parameters can be calculated as

$$\begin{aligned}\frac{1}{\eta_x} &= \left[\frac{\pi^2\mu^{2-\alpha}}{0.3}\Gamma\left(3-\frac{\alpha}{2}\right)\left(\frac{1}{3}-\frac{\bar{\Theta}_{\rm e}}{2}+\frac{\bar{\Theta}_{\rm e}^2}{5}\right)\frac{A(\alpha)\delta^2_{\rm R}}{R(\alpha)\delta^2_{\rm B}}\right]^{2/(6-\alpha)} \\ &\quad\times\left[1+\left(\frac{0.98}{N(\alpha)M(\alpha)}\frac{\delta^2_{\rm B}}{\mu^{2-\alpha}\delta^2_{\rm R}}\right)^{2/(6-\alpha)}\delta_{\rm R}^{4/(\alpha-2)}\right], \quad (24)\\ \eta_y &= \left[\frac{1.23\times\ln 2}{8\pi^2}\frac{(\alpha-2)R(\alpha)}{A(\alpha)\delta^2_{\rm R}}\right]^{2/(2-\alpha)} \\ &\quad\times\left[1+\left(\frac{0.51}{\ln 2}\delta^2_{\rm B}\right)^{2/(2-\alpha)}\right], \quad (25)\end{aligned}$$

where $\delta^2_{\rm B} = \mu^{2-\alpha}\delta^2_{\rm G}$ is the SI of GSM beam wave in weak anisotropic turbulence and is related to that in weak isotropic turbulence[20]

$$\begin{aligned}\delta^2_{\rm G} &= \frac{4\pi^2}{1.23}\frac{A(\alpha)}{R(\alpha)}\delta^2_{\rm R}\eta_l^{1-\alpha/2}\left\{\Gamma\left(1-\frac{\alpha}{2}\right){}_2{\rm F}_1\left(1-\frac{\alpha}{2},\frac{1}{2};\frac{3}{2};-\Lambda_{\rm e}\eta_l\right)+a_1\Gamma\left(\frac{3-\alpha}{2}\right)\right. \\ &\quad\times{}_2{\rm F}_1\left(\frac{3-\alpha}{2},\frac{1}{2};\frac{3}{2};-\Lambda_{\rm e}\eta_l\right)+a_2\Gamma\left(\frac{10-3\alpha}{4}\right){}_2{\rm F}_1\left(\frac{10-3\alpha}{4},\frac{1}{2};\frac{3}{2};-\Lambda_{\rm e}\eta_l\right) \\ &\quad-\frac{1}{T}\left[\frac{Z^{\alpha/2}}{\alpha}\Gamma\left(1-\frac{\alpha}{2}\right)\sin\left(\frac{\alpha}{2}\varphi_1+\varphi_2\right)+\frac{a_1Z^{(\alpha-1)/2}}{(\alpha-1)}\Gamma\left(\frac{3-\alpha}{2}\right)\sin\left(\frac{\alpha-1}{2}\varphi_1+\varphi_2\right)+\frac{a_2Z^{(3\alpha-6)/4}}{(3\alpha/2-3)}\Gamma\left(\frac{5}{2}-\frac{3\alpha}{4}\right)\right. \\ &\quad\left.\left.\times\sin\left(\frac{3\alpha-6}{4}\varphi_1+\varphi_2\right)\right]+\frac{\Lambda_{\rm e}\eta_l}{3{\rm T}^2}\left[\frac{1}{\alpha}\Gamma\left(1-\frac{\alpha}{2}\right)+\frac{a_1}{(\alpha-1)}\Gamma\left(\frac{3-\alpha}{2}\right)+\frac{a_2}{(3\alpha/2-3)}\Gamma\left(\frac{5}{2}-\frac{3\alpha}{4}\right)\right]\right\}, \quad (26)\end{aligned}$$

where

$$\begin{aligned}T &= \left[4(\Lambda_{\rm e}\eta_l)^2+(1+2\Theta_{\rm e})^2\eta_l^2\right]^{1/2}/6, \\ Z &= \left[(3+2\Lambda_{\rm e}\eta_l)^2+(1+2\Theta_{\rm e})^2\eta_l^2\right]^{1/2}/3, \\ \varphi_2 &= \tan^{-1}\left[2\Lambda_{\rm e}/(1+2\Theta_{\rm e})\right], \\ \varphi_1 &= \tan^{-1}\left[(1+2\Theta_{\rm e})\eta_l/(3+2\Lambda_{\rm e}\eta_l)\right].\end{aligned}$$

$$N(\alpha) = \frac{8\pi^2 A(\alpha)}{1.23R(\alpha)(\alpha-2)}\Gamma\left(\frac{6-\alpha}{\alpha-2}\right)B(\alpha)^{(6-\alpha)/(\alpha-2)}, \quad (27)$$

$$B(\alpha) = \frac{-\pi^2 4^{2-\alpha/2}\Gamma(1-\alpha/2)A(\alpha)}{1.23(\alpha-1)\Gamma(\alpha/2)R(\alpha)\bar{\Theta}_{\rm e}}, \quad (28)$$

$$\begin{aligned}M(\alpha) &= \int_0^1\xi^{\alpha-4}\left(1-\bar{\Theta}_{\rm e}\xi\right)^2 \\ &\quad\times\left[\left(1-\bar{\Theta}_{\rm e}\xi\right)^{\alpha-2}-\left(1-\bar{\Theta}_{\rm e}\right)^{\alpha-1}\right]^{(6-\alpha)/(2-\alpha)}{\rm d}\xi, \end{aligned} \quad (29)$$

The off-axis SI for an untracked GSM beam in moderate-to-strong anisotropic non-Kolmogorov turbulence[11] is given by

$$\begin{aligned}\delta^2_{\rm I,r}(r,L) &= U(\alpha)\mu^{2-\alpha}\delta^2_{\rm R}\Lambda_{\rm rec}^{\alpha/2-1}\left[r/W_{\rm LT}(L)\right]^2, \\ &\quad 0\leqslant r < W_{\rm LT}(L), \end{aligned} \quad (30)$$

$$U(\alpha) = \frac{4\pi^2}{1.23}\frac{\alpha-2}{1-\alpha}\Gamma\left(\frac{2-\alpha}{2}\right)\frac{A(\alpha)}{R(\alpha)}. \quad (31)$$

Considering additional beam wander and diffraction effects, the effective beam parameters are adopted by $\Lambda_{\rm rec} = 2L/\left[kW^2_{\rm LT}(L)\right]$; $W_{\rm LT}(L)$ is the long-term spot size for the GSM beam through anisotropic non-Kolmogorov turbulent atmosphere[22]

$$\begin{aligned}&W^2_{\rm LT}(L) \\ &\approx w_0^2+w_0^2\Lambda_0^2\zeta_{\rm s}+\frac{2}{3}\pi^2A(\alpha)\tilde{C}_n^2\mu^{-2}L^3 \\ &\quad\times\left\{\frac{\kappa_0^{4-\alpha}}{\Gamma(\alpha/2)}\left[\Gamma\left(\frac{\alpha}{2}-2\right)+a_1\frac{\kappa_0}{\kappa_l}\Gamma\left(\frac{5}{2}\right)\Gamma\left(\frac{\alpha}{2}-\frac{5}{2}\right)\right.\right. \\ &\quad\left.+a_2\left(\frac{\kappa_0}{\kappa_l}\right)^{3-\alpha/2}\Gamma\left(\frac{7}{2}-\frac{\alpha}{4}\right)\Gamma\left(\frac{3\alpha}{4}-\frac{7}{2}\right)\right] \\ &\quad+\kappa_l^{4-\alpha}\left[\Gamma\left(2-\frac{\alpha}{2}\right)+a_1\Gamma\left(\frac{5}{2}-\frac{\alpha}{2}\right)\right. \\ &\quad\left.\left.+a_2\,\Gamma\left(\frac{7}{2}-\frac{3\alpha}{4}\right)\right]\right\}. \end{aligned} \quad (32)$$

Based on equations (20), (21), and (30), the total SI of partially coherent GSM beams propagating through moderate-to-strong marine or terrestrial atmospheric turbulence can be

expressed as

$$\delta_{\mathrm{I}}^2(r,L) = U(\alpha)\mu^{2-\alpha}\frac{\Lambda_{\mathrm{rec}}^{\alpha/2-1}r^2\delta_{\mathrm{R}}^2}{W_{\mathrm{LT}}^2(L)} + \exp\left\{\frac{2\pi^2 A(\alpha)}{1.23R(\alpha)}\delta_{\mathrm{R}}^2\mu^{2-\alpha}\left(\frac{1}{3}-\frac{\bar{\Theta}_{\mathrm{e}}}{2}+\frac{\bar{\Theta}_{\mathrm{e}}^2}{5}\right)\right.$$
$$\times\left[\hat{\eta}_x^{3-\alpha/2}\left(\Gamma\left(3-\frac{\alpha}{2}\right)+a_1\Gamma\left(\frac{7}{2}-\frac{\alpha}{2}\right)\left(\frac{\hat{\eta}_x}{\eta_l}\right)^{1/2}\right.\right.$$
$$\left.+a_2\Gamma\left(\frac{9}{2}-\frac{3\alpha}{4}\right)\left(\frac{\hat{\eta}_x}{\eta_l}\right)^{3/2-\alpha/4}\right)$$
$$-\hat{\eta}_{x0}^{3-\alpha/2}\left(\Gamma\left(3-\frac{\alpha}{2}\right)+a_1\Gamma\left(\frac{7}{2}-\frac{\alpha}{2}\right)\left(\frac{\hat{\eta}_{x0}}{\eta_l}\right)^{1/2}\right.$$
$$\left.\left.+a_2\Gamma\left(\frac{9}{2}-\frac{3\alpha}{4}\right)\left(\frac{\hat{\eta}_{x0}}{\eta_l}\right)^{3/2-\alpha/4}\right)\right]$$
$$\left.+\frac{8\pi^2}{1.23}\frac{A(\alpha)}{R(\alpha)}\frac{\delta_{\mathrm{R}}^2}{\alpha-2}\eta_y^{1-\alpha/2}\right\}-1. \quad (33)$$

3. Numerical discussion

In this section, the numerical results of the SIs for partially coherent GSM beams propagating in a moderate-to-strong anisotropic non-Kolmogorov turbulent marine atmosphere are discussed. The following parameter values are assumed unless otherwise specified: anisotropy coefficient $\mu = 1.2$, power-spectrum index $\alpha = 3.8$, turbulence inner-scale $l_0 = 1$ mm, and outer-scale $L_0 = 1$ m, turbulence structure parameter $\widetilde{C}_n^2 = 5\times10^{-13}$ m$^{3-\alpha}$, propagation distance $L = 4$ km, wavelength $\lambda = 1550$ nm, beam width $w_0 = 1$ cm, phase curvature parameter $F_0 = 10$ km, and spatial correlation length $l_{\mathrm{s}} = 5$ cm.

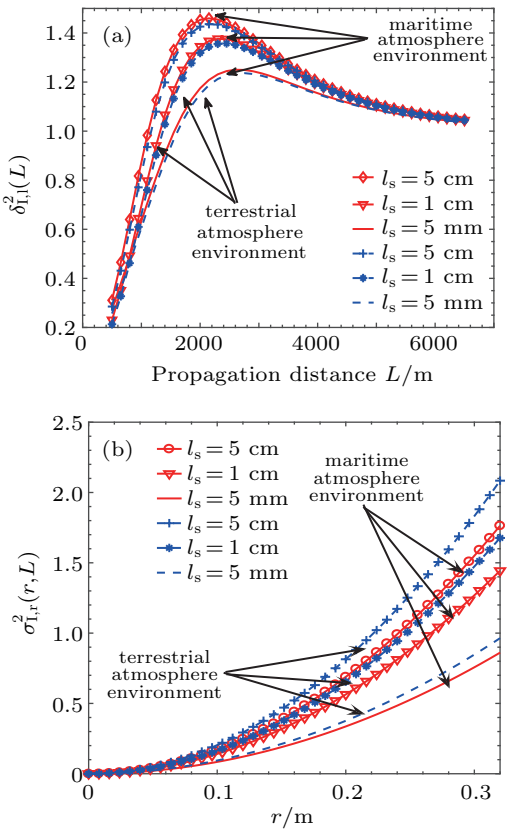


Fig. 1. (color online) On-axis (a) and off-axis (b) SIs of GSM beams versus L and r for different l_{s} in marine and terrestrial atmospheres.

Figure 1 shows the dependence of the on-axis (Fig. 1(a)) and off-axis (Fig. 1(b)) SIs of GSM beams through anisotropic non-Kolmogorov turbulence with source spatial coherence length l_{s}. A comparison of results in the marine and terrestrial atmosphere is also presented in Fig. 1. Both the on-axis and off-axis SIs for GSM beams are sensitive to the changes in l_{s}, and the negative effect of the turbulence on GSM beams can be reduced by decreasing the value of l_{s}. Partially coherent beams showed an obvious advantage over fully coherent ones in lowering the turbulence-induced SI. The on-axis SI in a turbulent marine atmosphere is higher than that in a turbulent terrestrial atmosphere. The result of the off-axis SI is different from that of the on-axis SI: terrestrial atmosphere produces a larger effect on the off-axis SI than the marine atmosphere.

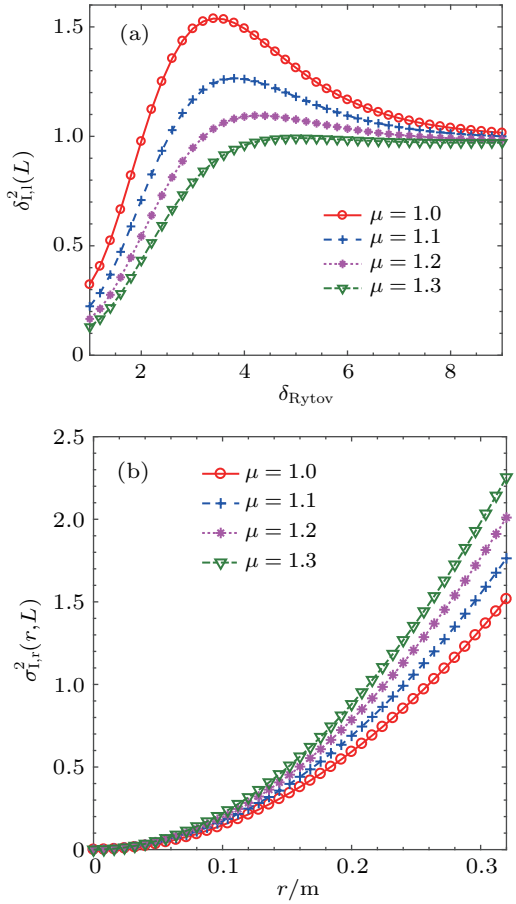


Fig. 2. (color online) On-axis (a) and off-axis (b) SIs of GSM beams versus δ_{R}^2 and r for different μ in the marine atmosphere.

The impact of the anisotropy coefficient μ ($\mu = 1$, 1.1, 1.2, and 1.3) on the on-axis (Fig. 2(a)) and off-axis (Fig. 2(b)) SIs of GSM beams in an anisotropic non-Kolmogorov marine atmosphere is investigated in Fig. 2. The on-axis SI of GSM beams increases with the turbulence strength until it reaches a maximum value in the focusing regime, where large-scale

inhomogeneity achieves its strongest effect; the on-axis SI enters the saturation decreasing regimes after reaching a maximum value because the focusing effect is weakened by multiple scattering in the turbulent saturation region. Atmospheric spatial coherence increases as the anisotropy parameter μ increases; the increase in μ leads to turbulent eddies acting as lenses with longer radii of curvature. A beam passing through an anisotropic turbulent eddy is less deviated from the direction of propagation and has a narrow spot size.[24] The point of large off-axis SI is closer to the beam center in anisotropic turbulence than that in isotropic turbulence. At a fixed position, the anisotropy characteristic of atmospheric turbulence leads to the decline in the on-axis SI and the rise in the off-axis SI. This effect is obvious in the moderate fluctuation regions for the on-axis SI, whereas for the off-axis SI, it is obvious at the positions far from the beam center.

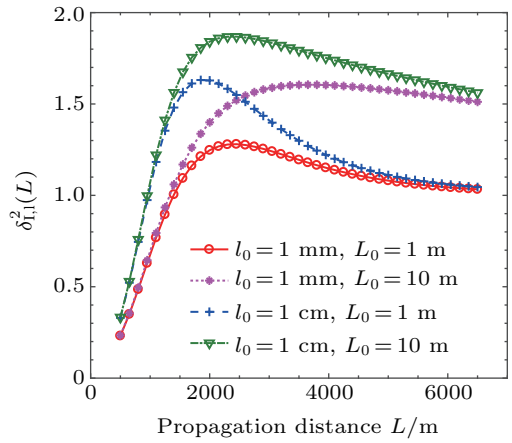


Fig. 3. (color online) On-axis SIs of GSM beams versus L for different l_0 and L_0 in the marine atmosphere.

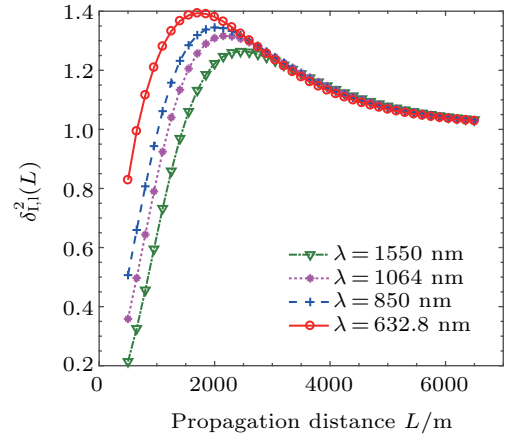


Fig. 4. (color online) On-axis SIs of GSM beams versus μ for different λ in the marine atmosphere.

Figure 3 depicts the influences of turbulence inner-scale l_0 and outer-scale L_0 on the on-axis SIs of GSM beams as a function of propagation distance L in an anisotropic non-Kolmogorov marine atmospheric turbulence. The curves of the on-axis SIs for different l_0 and L_0 values follow similar trends, but different values are obtained. Turbulence inner-scale has an important effect on the on-axis SIs in moderate fluctuation regions. Turbulence outer-scale plays a more important role in determining the strength of the on-axis SI in strong-turbulence regions. Both the turbulence inner-scale and outer-scale effects should be considered in the evaluation of the SI when the beam propagates in moderate-to-strong atmospheric turbulence.

Figure 4 illustrates the importance of wavelength λ on the on-axis SIs of GSM beams through an anisotropic non-Kolmogorov marine turbulent atmosphere as a function of L for $\lambda = 1550$, 1024, 850, and 632.8 nm. In weak-to-moderate turbulence regime, the on-axis SI increases with the decrease of λ; it trends toward a steady value when entering into the turbulence saturation phase. Wavelength also has a significant effect on the distance from the point (at which the maximum value is obtaining) to the source plane, a decreasing value of λ leads to a short distance.

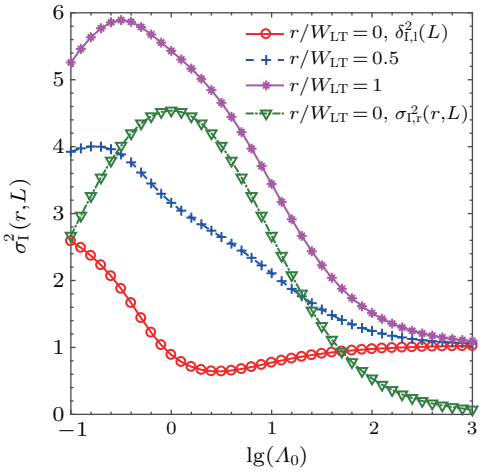


Fig. 5. (color online) SI of GSM beams versus $\Lambda_0$for different r in the marine atmosphere.

Figure 5 shows a plot of the total SIs of GSM beams in an anisotropic non-Kolmogorov marine turbulent atmosphere versus input beam parameter Λ_0 from 10^{-1} to 10^3 at a fixed propagation distance $L = 1$ km, where the effects of different values of the off-axis parameter r are considered. With the increase of Λ_0, the on-axis SI first decreases down to a trough and then begins to increase again. The curves of the off-axis SIs are different from the case of the on-axis SIs, which increase steeply to a peak value, and then decrease to zero. As $\Lambda_0 \to \infty$, GSM beams tend to be spherical waves, the on-axis SI of GSM beams is approximately equal to that of the spherical wave, and the off-axis SI disappears. The off-axis parameter r has a significant effect on the SIs of GSM beams in the vicinity of $\Lambda_0 = 1$ in a marine atmosphere.

Figures 6 exhibits the effect of power-spectrum index α on the SIs of GSM beams for $\alpha = 3.2$, 3.4, 3.6 to 3.8 in an anisotropic non-Kolmogorov marine turbulent atmosphere. The on-axis SI increases with the decrease of α in

the moderate-turbulence regime, which is consistent with the results in the weak turbulence regime.[20] whereas the on-axis SI enters into the turbulence saturation regime after reaching a maximum value, α has an opposite effect on it. Different values of α lead to obvious variations in the SIs which are away from the beam center.

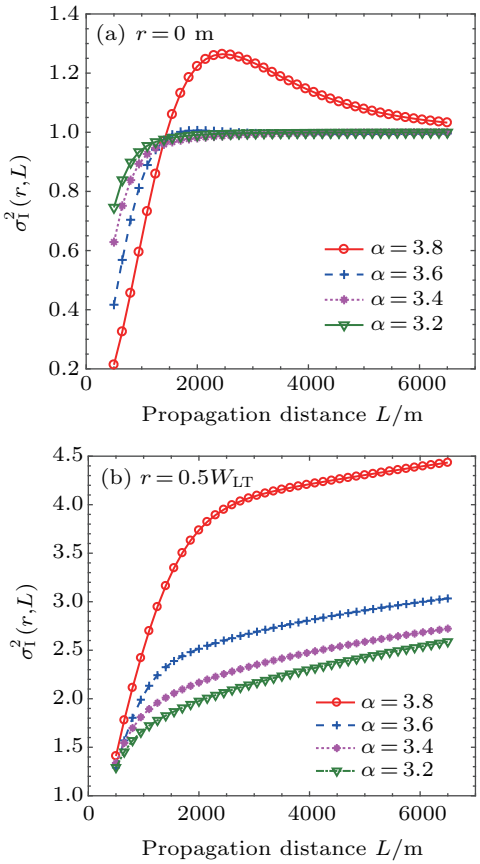


Fig. 6. (color online) SI of GSM beams versus L for different α and r in the marine atmosphere.

4. Conclusion

In conclusion, we have quantitatively investigated the SIs of GSM beams in a moderate-to-strong anisotropic non-Kolmogorov turbulent atmosphere. Both the on-axis and off-axis SIs of GSM beams in the turbulence were sensitive to changes in spatial correlation length; partially coherent beams showed an advantage over fully coherent ones in lowering the turbulence-induced SI. The on-axis SI in the marine atmosphere was higher than that in the terrestrial atmosphere, but the off-axis SI exhibited the opposite result. The anisotropy characteristic of turbulence led to a decline in the on-axis SI and a rise in the off-axis SI. Turbulence inner-scale had an obvious influence on the on-axis SI in moderate fluctuation regions, but the outer-scale effect was more apparent in strong-turbulence regions. The decrease in the on-axis SI induced by wavelength was remarkable in the moderate-to-strong. The on-axis SI initially increased with the turbulence strength, then began to decrease after reaching a maximum value. The on-axis SI increased with the decreasing power-spectrum index in the moderate-turbulence regime; it had the reverse effect in the saturation regime. The off-axis SIs strengthened as the off-axis parameter and propagation distance increased. With the increase in beam parameter Λ_0, the on-axis SI first decreased to a trough, and then began to increase again; the result of off-axis SI was opposite to that of the on-axis SI.

References

[1] Majumdar A K 2014 *Advanced Free Space Optics (FSO): A Systems Approach* (Springer)
[2] Andrews L C and Phillips R L 2005 *Laser Beam Propagation through Random Media* (SPIE Optical Engineering Press)
[3] Ricklin J C and Davidson F M 2003 *J. Opt. Soc. Am. A* **20** 856
[4] Gbur G and Wolf E 2014 *J. Opt. Soc. Am. A* **31** 2038
[5] Dogariu A and Amarande S 2003 *Opt. Lett.* **28** 10
[6] Korotkova O 2008 *Opt. Commun.* **281** 2342
[7] Miller W B, Ricklin J C and Andrews L C 1994 *J. Opt. Soc. Am. A* **11** 2719
[8] Andrews L C, Al-Habash M A, Hopen C Y and Phillips R L 2001 *Waves in Random Media* **11** 271
[9] Toselli I, Andrews L, Phillips R and Ferrero V 2009 *IEEE Trans. Antennas Propag.* **57** 1783
[10] Cui L, Xue B, Zheng S, Xue W, Bai X, Cao X and Zhou F 2011 *Opt. Express* **19** 16872
[11] Deng P, Yuan X and Huang D 2012 *Opt. Commun.* **285** 880
[12] Tan L Y, Zhai C, Yu S Y, Ma J and Lu G 2015 *Opt. Express* **23** 11250
[13] Li Y Q, Wu Z S, Zhang Y Y and Wang M J 2014 *Chin. Phys. B* **23** 074202
[14] Cang J and Liu X 2011 *Opt. Express* **19** 19067
[15] Deng P, Kavehrad M, Liu Z, Zhou Z and Yuan X 2013 *Opt. Express* **21** 15213
[16] Friehe C A, LaRue J C, Champagne F H, Gibson C H and Dreyer G F 1975 *J. Opt. Soc. Am. A* **65** 1502
[17] Grayshan K J, Vetelino F S and Young C Y 2008 *Waves in Random and Complex Media* **18** 173
[18] Cui L 2014 *J. Opt. Soc. Am. A* **31** 2030
[19] Baykal Y 2016 *J. Opt. Soc. Am. A* **33** 758
[20] Cheng M J, Guo L X and Zhang Y X 2015 *Opt. Express* **23** 32606
[21] Zhao Y, Zhang Y, Hu Z, Li Y and Wang D 2016 *Opt. Commun.* **371** 178
[22] Wu Y, Zhang Y and Hu Z 2016 *Progress in Electromagnetics Research M* **47** 141
[23] Cui L 2016 *Infrared Physics & Technology* **77** 431
[24] Toselli I, Agrawal B and Restaino S 2011 *J. Opt. Soc. Am. A* **28** 483
[25] Olver F W J 2010 *NIST Handbook of Mathematical Functions* (Cambridge University Press)
[26] Andrews L C 1998 *Special Functions of Mathematics for Engineers*, 2nd ed. (SPIE Optical Engineering Press)